$M(dmit)_2$ Salts with Nitronyl Nitroxide Radical Cations (M = Ni and Au, dmit = 1,3-Dithiol-2-thione-4,5-dithiolate). Nonmagnetic Single-Chain Formation vs Antiferromagnetic Spin-Ladder-Chain Formation of $M(dmit)_2$

Hiroyuki Imai,[†] Takeo Otsuka,[‡] Toshio Naito,[†] Kunio Awaga,[‡] and Tamotsu Inabe*,[†]

Contribution from the Division of Chemistry, Graduate School of Science, Hokkaido University, Sapporo 060-0810, Japan, and Department of Basic Science, Graduate School of Arts and Science, The University of Tokyo, Komaba, Meguro-ku, Tokyo 153-0041, Japan

Received April 2, 1999

Abstract: The crystal and magnetic structures of the 1:1 salts of $[M(dmit)_2]^-$ (M = Ni and Au) with the *p*-EPYNN (*p*-*N*-ethylpyridinium α-nitronyl nitroxide) cationic radical have been studied. Both crystals contain one-dimensional *p*-EPYNN chains with alternate head-to-tail orientation. In this chain a ferromagnetic interaction has been found to operate in common. Similarly, there is a common feature in the arrangement of $M(dmit)_2$; in both crystals $M(dmit)_2$ forms a one-dimensional chain through intermolecular S···S contacts between the outer rings of the ligand. However, a marked difference exists in the arrangement of these chains. The one-dimensional $Au(dmit)_2$ chain is sandwiched between the *p*-EPYNN chains, resulting in isolation of each one-dimensional $Au(dmit)_2$ chain. On the other hand, every two chains of $Ni(dmit)_2$ are sandwiched between the *p*-EPYNN chains, resulting in the $Ni(dmit)_2$ ladder-chain formation. In contrast to the absence of the unpaired electron in $[Au(dmit)_2]^-$, the presence of the unpaired electron in the frontier orbital of $[Ni(dmit)_2]^-$ plays an important role in the formation of an antiferromagnetic molecular spin ladder.

Introduction

Nitronyl nitroxide derivatives are known to show interesting magnetic properties when they form molecular crystals.[1] We have been paying particular attention to *N*-alkylated cationic derivatives of pyridyl nitronyl nitroxide (PYNN) radical. This unique "cation radical" prefers arrangements which are advantageous to ferromagnetic intermolecular interactions due to the electrostatic attraction between the oxygen atom in the NO group and the positively charged pyridinium ring. With varying the counterion, various crystal structures[2] including the *Kagomé* lattice[3] have been obtained.

We have expected that a unique molecular crystal may be obtained when the anionic part is constructed with π-radicals which can form a conduction path through the molecular overlap. In this case, there are two kinds of spin systems; one is a localized spin system in which the radical cation could magnetically interact with each other, and the other is a conduction electron system. For the purpose of constructing such a system, $Ni(dmit)_2$ anion is convenient, since the conduction paths can be formed not only along the π−π stacking direction

Chart 1

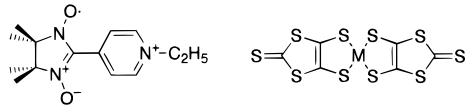

p-EPYNN $M(dmit)_2$

but also along the side-by-side direction due to the contacts between the peripheral sulfur atoms.[4] In the course of studying the structures and magnetic properties of the $Ni(dmit)_2$ salts with various *N*-alkylated PYNN cations, we have found that the $Ni(dmit)_2$ anion radical can form a ladder chain when the cation is *p*-EPYNN (*p*-*N*-ethylpyridinium α-nitronyl nitroxide).[5] The magnetic interaction between the $Ni(dmit)_2$ anion radicals is antiferromagnetic, and thus this compound was found to be the first example of the molecular antiferromagnetic spin ladder.

Recently, the ladder-type structure became a new target of the lattice architecture. Originally, the magnetic behavior of the antiferromagnetic spin-ladder system attracted attention; the appearance of the spin-gap depends on whether the number of legs in the ladder is even or odd.[6,7] In addition, holes doped into the two-leg ladders are predicted to pair and possibly superconduct.[6,8] Indeed, some cuprate which has two-leg ladder chains of copper oxide was found to achieve the superconducting

[†] Hokkaido University.
[‡] The University of Tokyo.

(1) Kinoshita, M. *Jpn. J. Appl. Phys.* **1994**, *33*, 5718.

(2) (a) Awaga, K.; Inabe, T.; Maruyama, Y.; Nakamura, T.; Matsumoto, M. *Chem. Phys. Lett.* **1992**, *195*, 21. (b) Yamaguchi, A.; Awaga, K.; Inabe, T.; Nakamura, T.; Matsumoto, M.; Maruyama, Y. *Chem. Lett.* **1993**, 1443. (c) Awaga, K.; Inabe, T.; Nakamura, T.; Matsumoto, M.; Maruyama, Y. *Mol. Cryst. Liq. Cryst.* **1993**, *232*, 69. (d) Awaga, K.; Yamaguchi, A.; Okuno, T.; Inabe, T.; Nakamura, T.; Matsumoto, M.; Maruyama, Y. *J. Mater. Chem.* **1994**, *4*, 1377.

(3) (a) Awaga, K.; Okuno, T.; Yamaguchi, A.; Hasegawa, M.; Inabe, T.; Maruyama, Y.; Wada, N. *Phys. Rev. B* **1994**, *49*, 3975. (b) N. Wada, N.; T. Kobayashi, T.; Yano, H.; Okuno, T.; Yamaguchi, A.; Awaga, K. *J. Phys. Soc. Jpn.* **1997**, *66*, 961.

(4) Cassoux, P.; Valade, L. In *Inorganic Materials*; Bruce, D. W., O'Hare, D., Eds.; John Wiley & Sons: Chichester, 1992; pp 2−58.

(5) Imai, H.; Inabe, T.; Otsuka, T.; Okuno, T.; Awaga, K. *Phys. Rev. B* **1996**, *54*, R6838.

(6) Rice, T. M.; Gopalan, S.; Sigrist, M. *Europhys. Lett.* **1993**, *23*, 445.

(7) (a) Azuma, M.; Hiroi, Z.; Takano, M.; Ishida, K.; Kitaoka, Y. *Phys. Rev. Lett.* **1994**, *73*, 3463. (b) Dagotto, E.; Rice, T. M. *Science* **1996**, *273*, 1515.

(8) Dagotto, E.; Riera, J.; Scalapino, D. J. *Phys. Rev. B* **1992**, *45*, 5744.

10.1021/ja991058k CCC: $18.00
Published on Web 08/19/1999

state under pressure.[9] In the molecular system, two more examples of the spin-ladder formation have been reported.[10,11] In all the cases including *p*-EPYNN[Ni(dmit)$_2$], the components of the ladder chain can interact with each other along both the plane-to-plane overlapping direction and the side-by-side S···S contacting direction. The rung in the ladder may be either of these two directions, and the leg in the ladder may be the other. In *p*-EPYNN[Ni(dmit)$_2$], the leg is formed by the S···S contacts, and the rung is formed by the plane-to-plane overlaps. Interestingly, when the Au(dmit)$_2$ anion, which has no unpaired electron, is combined with *p*-EPYNN, similar one-dimensional Au(dmit)$_2$ chains have been found to be formed by the S···S contacts. Each chain is, however, completely isolated, though the counter *p*-EPYNN cations form nearly the same one-dimensional chain as observed in *p*-EPYNN[Ni(dmit)$_2$]. In this paper, we describe the structures and magnetic properties of *p*-EPYNN[Ni(dmit)$_2$] and *p*-EPYNN[Au(dmit)$_2$], and discuss how the ladder-chain formation occurs only in *p*-EPYNN[Ni(dmit)$_2$].

Experimental Section

Materials. *p*-EPYNN·I was prepared according to the procedure previously reported.[2] *n*-Bu$_4$N[Ni(dmit)$_2$] was synthesized and purified following the method reported.[12] *n*-Bu$_4$N[Au(dmit)$_2$] was synthesized by a slightly modified method of the reported one[13] as follows. Under N_2 atmosphere a slight excess stoichiometric amount of methanol solution of sodium methoxide was added to an acetone solution of bis(benzoylthio)-1,3-dithiole-2-thione with stirring for 10 min. To this solution was added over a period of 15 min a slight less stoichiometric amount of $NaAuCl_4$ dissolved in a minimum amount of methanol . To the yellow-brown solution obtained after filtration was added a methanol solution of a stoichiometric amount of *n*-Bu$_4$N·I. The solution was concentrated under vacuum. Brown crystals of *n*-Bu$_4$N[Au(dmit)$_2$] were collected and recrystallized from acetone/methanol.

The simple salt crystals of *p*-EPYNN[M(dmit)$_2$] were prepared by the metathesis of *p*-EPYNN·I and *n*-Bu$_4$N[M(dmit)$_2$] in acetonitrile with slow diffusion in the H-tube at −2 to −10 °C. Black platelet crystals were obtained.

X-ray Structure Analyses. Automated MAC SCIENCE MXC18 (*p*-EPYNN[Ni(dmit)$_2$]) and Rigaku AFC-7R (*p*-EPYNN[Au(dmit)$_2$]) diffractometers with graphite-monochromated Mo Kα radiation were used for data collection at 296 K. The data-collection conditions are summarized in Table 1. Three standard reflections, which were monitored every 100 or 150 data measurements, showed no significant deviation in intensities. The structures were solved by a direct method (SIR-92,[14] *p*-EPYNN[Ni(dmit)$_2$]) and a Patterson method (*p*-EPYNN[Au(dmit)$_2$]), and the hydrogen atoms were placed at the calculated ideal positions. A full-matrix least-squares technique with anisotropic thermal parameters for non-hydrogen atoms and isotropic ones for hydrogen atoms (positions were not refined and the thermal parameters were refined for *p*-EPYNN[Ni(dmit)$_2$] and fixed (1.2 times of the attached carbons) for *p*-EPYNN[Au(dmit)$_2$]) was employed for the structure refinement.

Measurements. Static magnetic susceptibilities were measured in a field of 0.5 T on a Quantum Design MPMS-XL SQUID susceptometer. The temperature dependence of the magnetic susceptibility was examined in a range of 2−300 K. The correction for the diamagnetic contribution for *p*-EPYNN[Ni(dmit)$_2$] and *p*-EPYNN[Au(dmit)$_2$] was performed by using the diamagnetic susceptibilities that were evaluated assuming that the paramagnetic component follows the Curie law at a middle temperature range around 100 K. The corrected values were found to be consistent with the values expected from the Pascal's constants. The X-band EPR spectra were measured with randomly oriented polycrystalline samples on JEOL JES-FE1X and JES-RE2X spectrometers in the temperature range of 5−270 K. The electrical conductivity was measured with a two-probe method.

Table 1. Data-Collection Conditions and Crystal Data of *p*-EPYNN[Ni(dmit)$_2$] and *p*-EPYNN[Au(dmit)$_2$]

	p-EPYNN[Ni(dmit)$_2$]	*p*-EPYNN[Au(dmit)$_2$]
chemical formula	$C_{20}H_{21}N_3O_2S_{10}Ni$	$C_{20}H_{21}N_3O_2S_{10}Au$
molecular weight	714.70	852.97
crystal size/mm	0.50 × 0.25 × 0.20	0.50 × 0.20 × 0.05
crystal system	triclinic	triclinic
space group	$P\bar{1}$	$P\bar{1}$
a/Å	11.647(4)	14.420(5)
b/Å	11.986(3)	16.544(4)
c/Å	12.047(6)	12.741(3)
α/deg	103.25(3)	92.71(2)
β/deg	106.01(3)	100.13(2)
γ/deg	109.91(2)	103.61(2)
V/Å^3	1419.4(9)	2895(1)
Z	2	4
D_{calc}/g cm^{-3}	1.678	1.957
μ(Mo Kα)/cm^{-1}	14.19	58.45
2θ range	3° < 2θ < 55°	5° < 2θ < 55°
scan width/deg	1.20 + 0.30 tan θ	1.57 + 0.30 tan θ
scan mode	$\omega-2\theta$	$\omega-2\theta$
scan rate/deg min^{-1}	10	16
no. of reflcns measd	7059	13811
no. of independent reflcns obsed	4435 [$I > 3\sigma(I)$]	6687 [$I > 3\sigma(I)$]
no. of parameters	346	652
R	0.045	0.082
Rw	0.048	0.058

Results and Discussion

Crystal Structure of *p*-EPYNN[Ni(dmit)$_2$]. The crystal structure derived from X-ray structural analysis is shown in Figure 1. The crystal comprises two kinds of one-dimensional chains. Slightly nonplanar *p*-EPYNN (dihedral angle, 21.3° between the pyridinium ring and the ONCNO group) cation radicals are aligned along the *c*-axis, as shown in Figure 1b. This chain is slightly dimerized and one of the interatomic contacts within the dimer is extremely short: 2.948(7) Å between the nitronyl nitroxide oxygen and the pyridinium ring carbon. This is probably due to an electrostatic interaction between the negative charge on the oxygen and the positive charge on the pyridinium ring. Interatomic contacts between the dimers are not very short (the shortest between the oxygen and the pyridinium ring carbon is 3.331(7) Å), but the arrangement pattern is similar; the nitroxide oxygen is directed toward the pyridinium ring and there is no direct contacts between the nitroxide groups.

The molecular arrangement of Ni(dmit)$_2$ in this crystal is slightly different from those in ordinary Ni(dmit)$_2$ conductors. The shortest contacts exist between the molecules related by translation along the *c*-axis (Figure 1a). This direction is nearly parallel to the molecular plane, and one of the S···S contacts between the outer rings of the ligand is extremely short, 3.314(2) Å. By these contacts Ni(dmit)$_2$ forms a one-dimensional chain along the *c*-axis. In addition to this intermolecular interaction, there are ordinary plane-to-plane $\pi-\pi$ overlaps. However, this interaction is restricted only within two chains. The one-dimensional *p*-EPYNN chain overlaps with one side of the

(9) Uehara, U.; Nagata, T.; Akimitsu, J.; Takahashi, H.; Mori, N.; Kinoshita, K. *J. Phys. Soc. Jpn.* **1996**, *65*, 2764.
(10) Komatsu, T.; Kojima, N.; Saito, G. *Solid State Commun.* **1997**, *103*, 519.
(11) Rovira, G.; Veciana, J.; Ribera, E.; Tarrés, J.; Canadell, E.; Rousseau, R.; Mas, M.; Molins, E.; Almeida, M.; Henriques, R. T.; Morgado, J.; Schoeffel, J.-P.; Pouget, J.-P. *Angew. Chem., Int. Ed. Engl.* **1997**, *36*, 2324.
(12) Steimecke, G.; Sieler, H. J.; Kirmse, R.; Hoyer, E. *Phosphorus Sulfur* **1979**, *7*, 49.
(13) Kirmse, R.; Stach, J.; Dietzsch, W.; Steimecke, G.; Hoyer, E. *Inorg. Chem.* **1980**, *19*, 2679.
(14) Altomare, A.; Burla, M. C.; Camalli, M.; Cascarano, M.; Giacovazzo, C.; Guagliardi, A.; Polidori, G. *J. Appl. Cryst.* **1994**, *27*, 435.

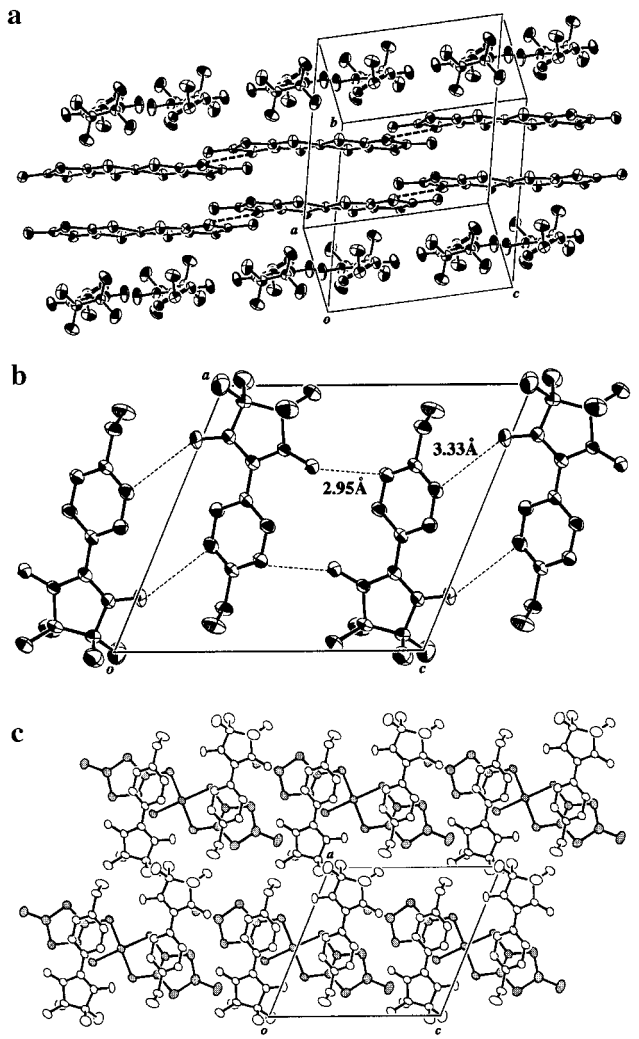

Figure 1. Crystal structure of *p*-EPYNN[Ni(dmit)$_2$]: overall view of the one-dimensional *p*-EPYNN chains and the Ni(dmit)$_2$ ladder chain (a), molecular arrangement in the *p*-EPYNN chain (b), and view perpendicular to the Ni(dmit)$_2$ molecular plane (c). The broken lines in part a indicate the short S···S contacts.

Ni(dmit)$_2$ plane. Since there is an inversion center between the plane-to-plane overlapped Ni(dmit)$_2$ molecules, the inverse situation occurs on another Ni(dmit)$_2$ chain. Consequently, the Ni(dmit)$_2$ ladder chain is sandwiched by the one-dimensional *p*-EPYNN chains. As can be seen from Figure 1c, inter-ladder contact along the *a*-axis is practically negligible; the shortest S···S contact between the ladder chains is 4.028(2) Å, which is much larger than twice the van der Waals radius (1.85 Å). This isolation of each ladder chain is realized by the terminal ethyl group and four methyl groups of *p*-EPYNN, which surround the ladder chain. Intermolecular contacts between the plane-to-plane overlapped Ni(dmit)$_2$ molecules are not so short; the interplanar distance is 3.73 Å.

Since [Ni(dmit)$_2$]$^-$ is a π-radical, some electron delocalization is expected to occur. From the ladder structure, it is expected to be most effective along the *c*-axis. Actually, the conductivity along the *c*-axis is found to be highest, 1.3×10^{-4} Ω^{-1} cm^{-1} at room temperature. The temperature dependence is semiconducting with the activation energy of 0.27 eV. On the other hand, the conductivity perpendicular to the *c*-axis in the *ac*-plane is much less, 4×10^{-7} Ω^{-1} cm^{-1} at room temperature.

Crystal Structure of *p*-EPYNN[Au(dmit)$_2$]. The crystal structure of *p*-EPYNN[Au(dmit)$_2$] is shown in Figure 2. This crystal also belongs to the triclinic $P\bar{1}$ space group. However,

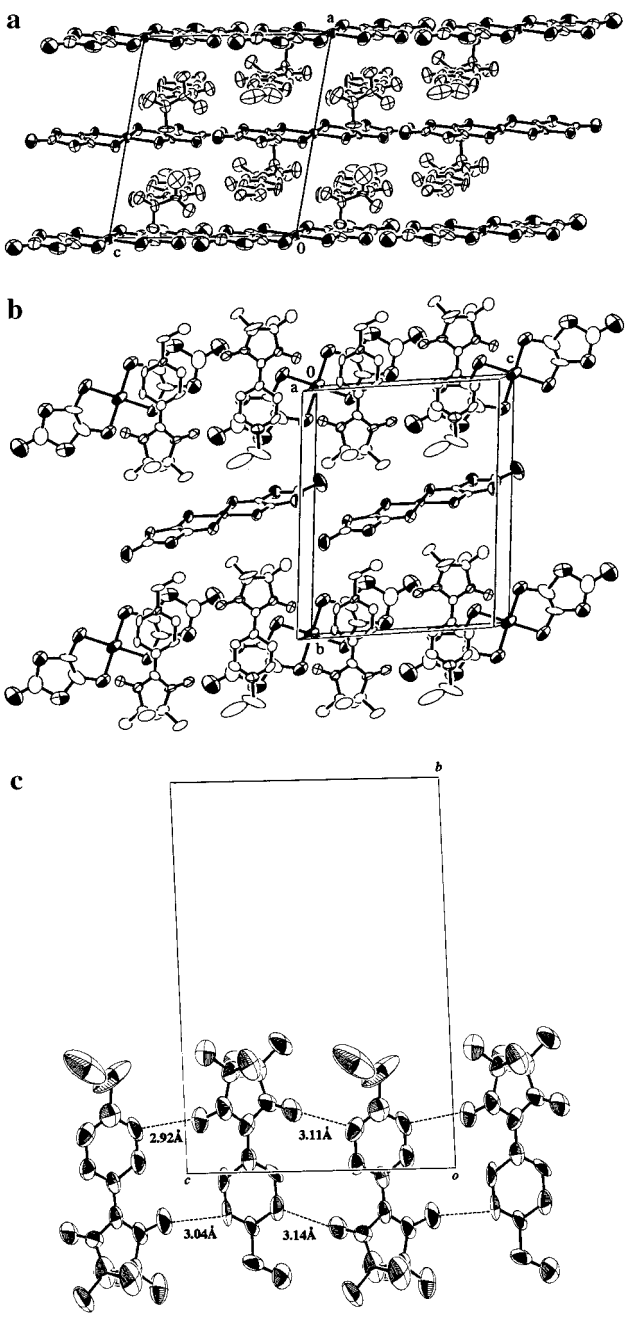

Figure 2. Crystal structure of *p*-EPYNN[Au(dmit)$_2$]: view along the *b*-axis (a, Au(dmit)$_2$ at the general position is omitted), view perpendicular to the Au(dmit)$_2$ molecular plane (b, $0 < x < 1/2$), and molecular arrangement in the *p*-EPYNN chain (c).

the unit cell contains four *p*-EPYNN[Au(dmit)$_2$] formulas. There are two Au atoms on the inversion center (both are of 1/2 occupancy) and one Au atom on a general position. Consequently two *p*-EPYNN cations and two halves and one [Au(dmit)$_2$] units constitute the asymmetric unit.

Figure 2a shows a projection of the structure along the *b*-axis. There is a one-dimensional chain of the *p*-EPYNN cations along the *c*-axis, of which molecular arrangement is practically the same as that observed in the Ni(dmit)$_2$ salt. Since the two crystallographically independent *p*-EPYNN radicals form the one-dimensional chain, there are two pairs of intermolecular contacts between the nitronyl nitroxide oxygen and the pyridinium ring carbon (Figure 2c). One pair is shorter than the other: 2.92(2) and 3.04(3) Å vs 3.11(2) and 3.14(3) Å. This

slightly dimerized feature is also similar to the *p*-EPYNN chain in the Ni salt, though the interdimer contacts are shorter in the Au salt.

The arrangement of part of the Au(dmit)$_2$ anions has some similarity to that of the Ni salt (Figure 2, a and b). The Au(dmit)$_2$ anions at (0,0,0) and (0.5,0,0) form one-dimensional chains, respectively, along the *c*-axis with moderately short S···S contacts between the outer rings of the ligand. The shortest S···S distances are 3.49(2) and 3.45(1) Å, respectively, which are longer than that in the Ni salt. A marked difference from the Ni salt lies in the arrangement of the one-dimensional M(dmit)$_2$ chains. In the Ni salt, the one-dimensional *p*-EPYNN chain overlaps only one side of the M(dmit)$_2$ plane, resulting in the ladder chain formation. In the Au salt, the one-dimensional *p*-EPYNN chain similarly overlaps with the M(dmit)$_2$ plane. However, the overlaps occur on both sides of the M(dmit)$_2$ plane, and each single one-dimensional Au(dmit)$_2$ chain is isolated. Since the Au(dmit)$_2$ anion does not carry any unpaired electron, no exchange energy gain is attained by close contacts between the Au(dmit)$_2$ anions. Therefore, no driving force toward face-to-face overlapping or close S···S contacts between the Au(dmit)$_2$ anions operates in the crystal of *p*-EPYNN[Au(dmit)$_2$]. To neutralize the charge, an additional one-dimensional Au(dmit)$_2$ chain locates along the *c*-axis with similar S···S contacts (the shortest is 3.525(8) Å) between the outer rings of the ligand. The molecular plane in this chain is nearly perpendicular to that in the chain sandwiched by the *p*-EPYNN chains. Interchain contacts in the *ac*-plane are rather weak; the S···S distances are >3.68 Å.

Magnetic Susceptibilities of *p*-EPYNN[Ni(dmit)$_2$] and *p*-EPYNN[Au(dmit)$_2$]. The obtained paramagnetic susceptibility, χ_P, of *p*-EPYNN[Au(dmit)$_2$] is shown in Figure 3a, where $\chi_P T$ vs T is plotted. In this salt, the radical species is restricted to *p*-EPYNN which arranges in a similar way with that found in the Ni salt. It is worth noting that $\chi_P T$ upturns at low temperature more than the value expected for the $S = 1/2$ Curie spins. This clearly indicates that a ferromagnetic interaction operates between the *p*-EPYNN radical cations. The *p*-EPYNN radical cations are aligned in a one-dimensional chain without effective contacts between the nitronyl nitroxide groups. This alignment pattern satisfies the empirical condition for a ferromagnetic coupling. The susceptibility of this component can thus be analyzed using the following equation for the one-dimensional ferromagnetic chain,[15]

$$\chi_P(T) = \frac{C}{T}\left(\frac{1 + A_1K + A_2K^2 + A_3K^3 + A_4K^4 + A_5K^5}{1 + A_6K + A_7K^2 + A_8K^3 + A_9K^4}\right)^{2/3}$$

with $K = J/2k_BT$, where J is the ferromagnetic exchange coupling constant of *p*-EPYNN, k_B is the Boltzmann constant, and C corresponds to the Curie constants for *p*-EPYNN. The parameters A_1-A_9 are defined in the literature.[15] The best fit obtained for *p*-EPYNN[Au(dmit)$_2$] with the parameters $C = 0.375$ (fixed) and $J/k_B = 0.38$ K is depicted as a solid curve in Figure 3a. The small anomaly around 50 K is probably due to the adsorbed oxygen on the crystal surfaces.

On the other hand, in the $\chi_P T$ vs T plot of *p*-EPYNN[Ni(dmit)$_2$] shown in Figure 3b, there are two distinct temperature dependencies. One is above 150 K, increase of $\chi_P T$ with increasing temperature, and another is below 40 K, increase of $\chi_P T$ with decreasing temperature. The behavior at low temperature is quite similar to that observed for *p*-EPYNN[Au(dmit)$_2$], and it has been found in both crystal structures that *p*-EPYNN arranges in a similar way. Therefore, the observed susceptibility is considered to consist of the contribution from the ferromagnetically interacting one-dimensional *p*-EPYNN chains and that from a thermally activated species which is nonmagnetic at lower temperature. From the crystal structure, the latter magnetic contribution is reasonably assigned to the spin-ladder chains of the Ni(dmit)$_2$ radical anions, since such an antiferromagnet produces spin-gap. Therefore, the paramagnetic susceptibility of *p*-EPYNN[Ni(dmit)$_2$] can be analyzed by a sum of the term of the spin-ladder chain[16] and that of the one-dimensional ferromagnetic chain as follows,

$$\chi_P(T) = \frac{2C_1}{\sqrt{\pi(a/k_B)T}}e^{-\Delta/k_BT} + \frac{C_2}{T}\left(\frac{1 + A_1K + A_2K^2 + A_3K^3 + A_4K^4 + A_5K^5}{1 + A_6K + A_7K^2 + A_8K^3 + A_9K^4}\right)^{2/3}$$

The parameter Δ is the magnetic gap and $a = {}^1/_2[\partial^2\epsilon(k)/\partial k^2]_{k=\pi}$, where $\epsilon(k)$ is the energy dispersion of the spin wave excitation in the spin ladder of [Ni(dmit)$_2$], and C_1 and C_2 correspond to the Curie constants for [Ni(dmit)$_2$] and *p*-EPYNN, respectively. The solid curve in Figure 3b represents the best fit of the experimental data obtained with $\Delta/k_B = 940$ K, $a/k_B = 13.6$ K, and $J/k_B = 0.16$ K. The parameters C_1 and C_2 are fixed as $C_1 = 0.394$ emu K mol^{-1} ($g = 2.05$) and $C_2 = 0.375$ emu K mol^{-1} ($g = 2.00$). The bright and dark shaded parts in the figure show the contributions of [Ni(dmit)$_2$] and *p*-EPYNN, respectively. The broken curve is the theoretical trial fit using the simple dimer model with $\Delta/k_BT = 870$ K, which manifests significant deviation from the experimental plots.

The smaller J/k_B value in the Ni salt compared with the Au salt is consistent with the structural data. The intra- and interdimer contacts between the nitronyl nitroxide oxygen and the pyridinium ring carbons in the one-dimensional *p*-EPYNN chain are always closer in the Au salt than in the Ni salt.

The assignment of the two paramagnetic components in *p*-EPYNN[Ni(dmit)$_2$] was also checked by the EPR spectroscopy. In the temperature region measured, a single absorption signal was observed. However, as shown in Figure 4, the average *g*-value and the line width at half-height of the absorption peak show large temperature dependence. At low temperatures, a sharp absorption signal with the *g*-value close to those of typical nitronyl nitroxide radicals was observed. Below 150 K, both *g*-value and line width are almost constant. A marked increase of the *g*-value and line width starts at ~150 K. Since both relatively large *g*-value and line width are characteristics of the [Ni(dmit)$_2$]$^-$ radical, the observed temperature dependence indicates that a paramagnetic contribution from the [Ni(dmit)$_2$]$^-$ radical is almost negligible at low temperature and becomes significant above ~150 K. The observation is quite consistent with the interpretation of the temperature dependence of the susceptibility.

Formation of the Spin-Ladder Chain in *p*-EPYNN[Ni(dmit)$_2$]. It has been clearly indicated that the spin-ladder chain of the Ni(dmit)$_2$ radical anion coexists with the ferromagnetic one-dimensional chain of the *p*-EPYNN radical cation in *p*-EPYNN[Ni(dmit)$_2$]. In *p*-EPYNN[Au(dmit)$_2$], the *p*-EPYNN radical cation has been found to form nearly the same one-dimensional chain as that observed in *p*-EPYNN[Ni(dmit)$_2$]. Indeed, this one-dimensional alignment of PYNN was also found in the simple iodide salt of the *p*-*N*-*n*-butyl PYNN derivative,[2d]

(15) Kahn, O. In *Molecular Magnetism*; VCH Publishers, Inc.: New York, 1993; Chapter 11.

(16) Troyer, M.; Tsunetsugu, H.; Warts, D. *Phys. Rev. B* **1994**, *50*, 13515.

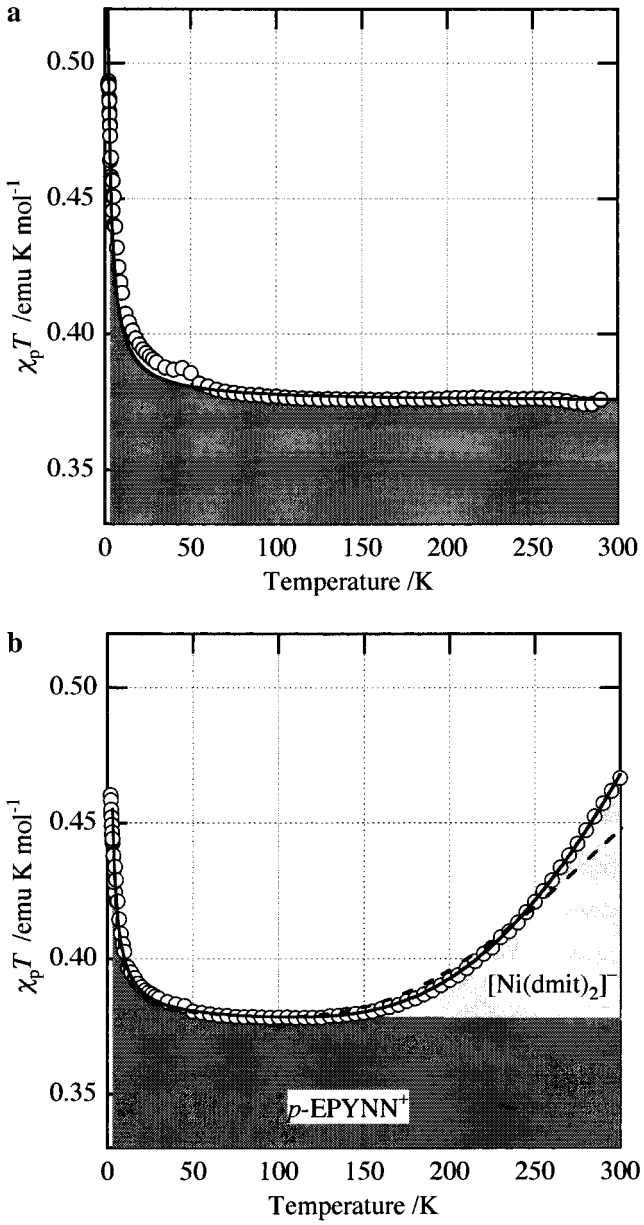

Figure 3. Temperature dependence of the paramagnetic susceptibility (χ_p) of *p*-EPYNN[Au(dmit)$_2$] (a) and *p*-EPYNN[Ni(dmit)$_2$] (b). The solid lines are the theoretical fit using equations in the text. The thick and bright regions in part b represent the contribution from *p*-EPYNN and Ni(dmit)$_2$, respectively. The broken line in part b is the trial best fit using a simple dimer model.

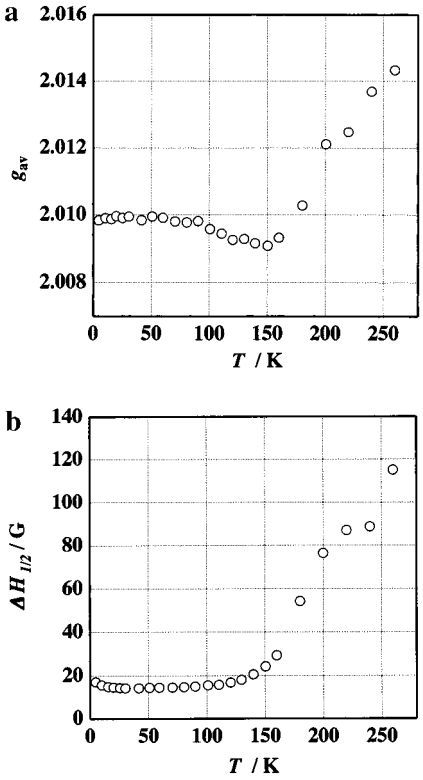

Figure 4. Temperature dependence of the average *g* value (g_{av}) (a) and the half-height line width ($\Delta H_{1/2}$) (b) observed by EPR of the randomly oriented *p*-EPYNN[Ni(dmit)$_2$] polycrystalline sample.

and seems to be favorable for the *p-N*-alkylated PYNN derivatives. The combination of this one-dimensionally interacting component and the two-dimensionally interacting Ni(dmit)$_2$ anion radical may lead to the ladder-chain formation, which is intermediate between one and two dimensions. On the other hand, in *p*-EPYNN[Au(dmit)$_2$], for lack of the transfer energy gain between the Au(dmit)$_2$ anions due to the absence of the unpaired electron, each one-dimensional Au(dmit)$_2$ chain has no interaction with the other chains.

Finally, the transfer energy gain in *p*-EPYNN[Ni(dmit)$_2$] has been evaluated from an extended Hückel calculation. The molecular orbital of [Ni(dmit)$_2$]$^-$ accommodating the unpaired electron, generally called LUMO, has small coefficients at the outer rings of the ligand.[17] In addition, the signs on the S atoms are alternately inverse. The S···S contacts along the one-dimensional Ni(dmit)$_2$ chain observed in *p*-EPYNN[Ni(dmit)$_2$] are thus not efficient in terms of the transfer energy; the overlap integral is only 0.13×10^{-3}. On the other hand, the overlap integral between the plane-to-plane overlapped Ni(dmit)$_2$ molecules has been found to be significantly large, -17.0×10^{-3}, though the interplanar distance is relatively large (3.73 Å). Since the transfer integral (t) is approximately proportional to the overlap integral, the transfer energy gain between the plane-to-plane overlapped Ni(dmit)$_2$ molecules is supposed to dominate the ladder chain formation in *p*-EPYNN[Ni(dmit)$_2$].

This information about the transfer integrals is also of use to evaluate the magnetic exchange interaction in the ladder chain. Since the exchange energy, J, is proportional to t^2, in *p*-EPYNN-[Ni(dmit)$_2$] $J_\perp$ (exchange energy in the rung of the ladder) is about 10 thousand times larger than $J_\parallel$ (exchange energy in the leg of the ladder). Thus, the observed large gap energy (940 K) is predominantly involved with the antiferromagnetic interaction in the plane-to-plane overlapped Ni(dmit)$_2$ dimer. The observed relatively high conductivity for a half-filled insulator, however, suggests that the interaction along the leg may possibly be larger than that estimated. Though the precise values of $J_\perp$ and $J_\parallel$ in the spin ladder are important for characterizing the electronic and magnetic structure, their experimental determination is generally difficult. The successful determination was reported for a spin ladder composed of a binuclear Cu^{2+} complex, in which the gap energy is relatively small.[18] For spin ladders with much larger gap energy, more elaborate work may be required.

The carrier doping in the spin ladder may be another attractive subject. The doping in *p*-EPYNN[Ni(dmit)$_2$] was attempted by

(17) Kobayashi, A.; Kim, H.; Sasaki, Y.; Kato, R.; Kobayashi, H. *Solid State Commun.* **1987**, *62*, 57.

(18) (a) Chaboussant, G.; Crowell, P. A.; Lévy, L. P.; Piovesana, O.; Madouri, A.; Mailly, D. *Phys. Rev. B* **1997**, *55*, 3046. (b) Chaboussant, G.; Julien, M.-H.; Fagot-Revurat, Y.; Lévy, L. P.; Berthier, C.; Horvatic, M.; Piovesana, O. *Phys. Rev. Lett.* **1997**, *79*, 925.

growing crystals under coexistence of some dopants which are expected to replace a part of the cations. The obtained crystals showed no effect of doping, and the dopants were probably not incorporated in the lattice. On the other hand, replacement of a part of the [Ni(dmit)$_2$] ladder by [Au(dmit)$_2$] has been found to be possible, and a study of the resulting magnetic properties is now under way.

Acknowledgment. This work was partly supported by the Grant-In-Aid for Scientific Research from the Ministry of Education, Science, and Culture of the Japanese government and by the CREST (Core Research for Evolutional Science and Technology) of the Japan Science and Technology Corporation (JST).

Supporting Information Available: Tables of crystal data, structure solution and refinement, atomic coordinates, bond lengths and angles, and anisotropic thermal parameters for *p*-EPYNN[Ni(dmit)$_2$] and *p*-EPYNN[Au(dmit)$_2$] (PDF) and X-ray files (CIF). This material is available free of charge via the Internet at http://pubs.acs.org.

JA991058K